NASA/TM—2019–000000

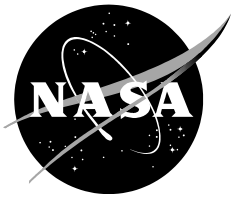

TESS Data Release Notes:
Sector 8, DR10

Michael M. Fausnaugh, Christopher J. Burke
Kavli Institute for Astrophysics and Space Science, Massachusetts Institute of Technology, Cambridge, Massachusetts

Douglas A. Caldwell
SETI Institute, Mountain View, California

Jon M. Jenkins
Ames Research Center, Moffett Field, California

Jeffrey C. Smith, Joseph D. Twicken
SETI Institute, Mountain View, California

Roland Vanderspek
Kavli Institute for Astrophysics and Space Science, Massachusetts Institute of Technology, Cambridge, Massachusetts

John P. Doty
Noqsi Aerospace Ltd, Billerica, Massachusetts

Eric B. Ting
Ames Research Center, Moffett Field, California

Joel S. Villasenor
Kavli Institute for Astrophysics and Space Science, Massachusetts Institute of Technology, Cambridge, Massachusetts

April 11, 2019

Acknowledgements

These Data Release Notes provide information on the processing and export of data from the Transiting Exoplanet Survey Satellite (TESS). The data products included in this data release are full frame images (FFIs), target pixel files, light curve files, collateral pixel files, cotrending basis vectors (CBVs), and Data Validation (DV) reports, time series, and associated xml files.

These data products were generated by the TESS Science Processing Operations Center (SPOC, Jenkins et al., 2016) at NASA Ames Research Center from data collected by the TESS instrument, which is managed by the TESS Payload Operations Center (POC) at Massachusetts Institute of Technology (MIT). The format and content of these data products are documented in the Science Data Products Description Document (SDPDD)[1]. The SPOC science algorithms are based heavily on those of the Kepler Mission science pipeline, and are described in the Kepler Data Processing Handbook (Jenkins, 2017).[2] The Data Validation algorithms are documented in Twicken et al. (2018) and Li et al. (2019). The TESS Instrument Handbook (Vanderspek et al., 2018) contains more information about the TESS instrument design, detector layout, data properties, and mission operations.

The TESS Mission is funded by NASA's Science Mission Directorate.

This report is available in electronic form at
https://archive.stsci.edu/tess/

[1] https://archive.stsci.edu/missions/tess/doc/EXP-TESS-ARC-ICD-TM-0014.pdf
[2] https://archive.stsci.edu/kepler/manuals/KSCI-19081-002-KDPH.pdf

1 Observations

TESS Sector 8 observations include physical orbits 23 and 24 of the spacecraft around the Earth. The use of Camera 1 in attitude control was disabled at the start of both orbits due to strong scattered light signals. At TJD 1531.74, an interruption in communications between the instrument and spacecraft occurred, resulting in an instrument turn-off until TJD 1535.00. No data or telemetry were collected during this period. Data collection was paused for 1.19 days during perigee passage while downloading data. In total, there are 20.22 days of science data collected in Sector 8.

Table 1: Sector 8 Observation times

	UTC	TJD[a]	Cadence #
Orbit 23 start	2019-02-02 20:09:35	1517.34150	208718
Camera 1 guiding enabled	2019-02-02 21:27:35	1517.39566	208757
Orbit 23 end	2019-02-14 13:31:35	1529.06510	217159
Orbit 24 start	2019-02-15 18:09:35	1530.25816	218018
Camera 1 guiding enabled	2019-02-15 22:41:35	1530.44705	218154
Instrument anomaly start	2019-02-17 05:48:35	1531.74288	221434
Data collection resumed	2019-02-20 12:02:38	1535.00264	221432
Orbit 24 end	2019-02-27 11:57:34	1541.99982	226472

[a] TJD = TESS JD = JD - 2,457,000.0

The spacecraft was pointing at RA (J2000): 128.1156°; Dec (J2000): −37.7370°; Roll: 155.3091°. Two-minute cadence data were collected for 20,000 targets, and full frame images were collected every 30 minutes. See the TESS project Sector 8 observation page[3] for the coordinates of the spacecraft pointing and center field-of-view of each camera, as well as the detailed target list. Fields-of-view for each camera and the Guest Investigator two-minute target list can be found at the TESS Guest Investigator Office observations status page[4].

1.1 Notes on Individual Targets

Six very bright stars (Tmag $\lesssim$ 2) with large pixel stamps were not processed in the photometric pipeline. Target pixel files with raw data are provided, but no light curves were produced. The affected TIC IDs are 134501440, 38877693, 31975064, 255559489, 46799297, 238001475.

Two stars (300015238 and 354825493) had very bright unresolved stars nearby (300015239 and 354825513 respectively). The contaminating flux for these objects is very large and the pipeline assigns them an incorrect photometric aperture. In general, the quality of the resulting photometry for such targets is expected to be poor in light of the contamination.

Two targets (342884451 and 269407223) had apertures selected (25x25 pixels) that did not fully capture the bleed trails.

[3] https://tess.mit.edu/observations/sector-8

[4] https://heasarc.gsfc.nasa.gov/docs/tess/status.html

1.2 Spacecraft Pointing and Momentum dumps

The reaction wheel speeds were reset with momentum dumps every 3.125 days. Figure 1 summarizes the pointing performance over the course of the sector based on Fine Pointing telemetry.

At the start of each orbit, the Earth was close to the boresight of Camera 1, and the level of scattered light was too high for meaningful guide star centroids to be measured. Guiding with Camera 1 was therefore disabled at these times. When Camera 1 guiding was re-enabled, the spacecraft attitude shifted by a small amount, about 1 arc-second (0.05 pixels). These times are marked with Attitude Tweak flags in the data products.

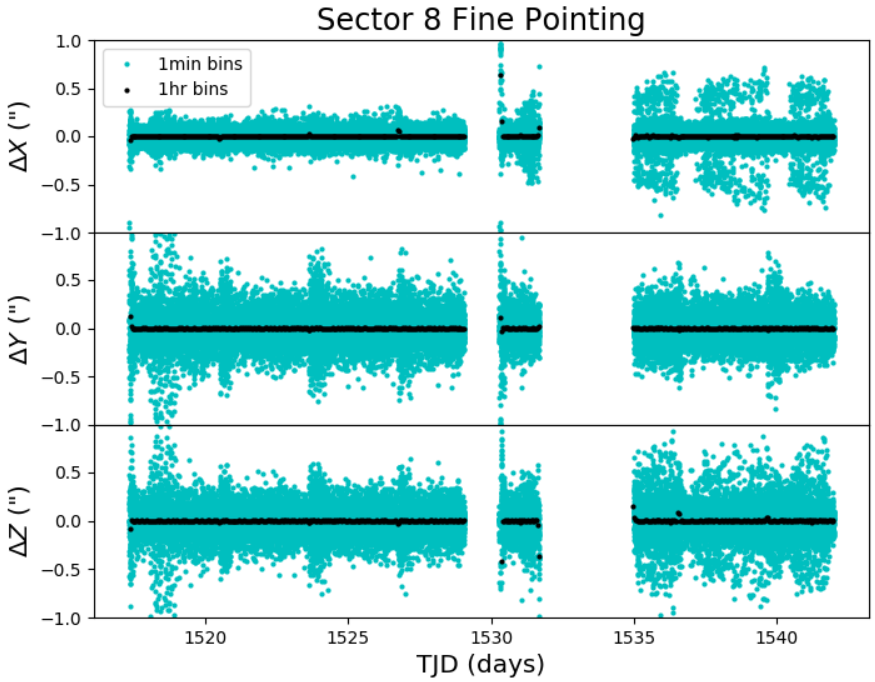

Figure 1: Guiding corrections based on spacecraft fine pointing telemetry. The delta-quaternions from each camera have been converted to spacecraft frame, binned to 1 minute and 1 hour, and averaged across cameras. Long-term trends (such as those caused by differential velocity aberration) have also been removed. The ΔX/ΔY directions represent offsets along the the detectors' rows/columns, while the ΔZ direction represents spacecraft roll.

1.3 Scattered Light

Figure 2 shows the median value of the background estimate for all targets on a given CCD as a function of time. Figure 3 shows the angle between each camera's boresight and the Earth or Moon—this figure can be used to identify periods affected by scattered light and the relative contributions of the Earth and Moon to the image backgrounds. In Sector 8, the main stray light features are caused by the Earth at the start of each orbit, and the Moon in Camera 1 towards the start of orbit 24.

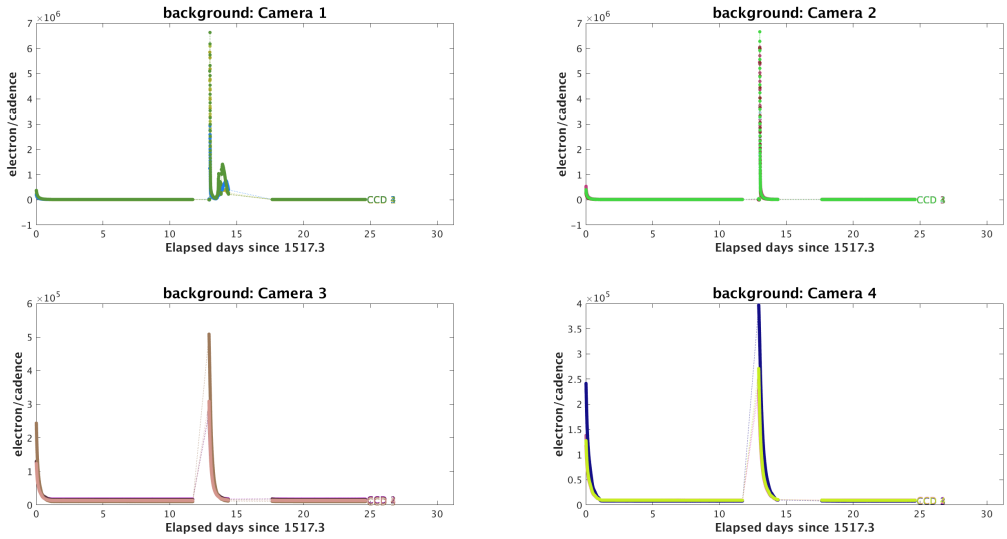

Figure 2: Median background flux across all targets on a given CCD in each camera. The changes are caused by variations in the orientation and distance of the Earth and Moon.

2 Data Anomaly Flags

See the SDPDD (§9) for a list of data quality flags and the associated binary values used for TESS data, and the Instrument Handbook for a more detailed description of each flag.

The following flags were not used in Sector 8: bits 7, 9, and 11 (Cosmic Ray in Aperture, Discontinuity, Cosmic Ray in Collateral Pixel).

Cadence 221429, when data collection resumed after the instrument anomaly, was marked with bit 2 (Safe Mode). This was done only for data processing purposes (see §4.2).

Cadences marked with bits 1, 3, 4, 6, and 12 (Attitude Tweak, Coarse Point, Earth Point, Reaction Wheel Desaturation Event, and Straylight) were marked based on spacecraft telemetry.

Cadences marked with bit 5 and 10 (Argabrightening Events and Impulsive Outlier) were identified by the SPOC pipeline. Bit 5 marks a sudden change in the background measurements. In practice, bit 5 flags are caused by rapidly changing glints and unstable pointing at times near momentum dumps. Bit 10 marks an outlier identified by PDC and omitted from the cotrending procedure.

Cadences marked with bit 8 (Manual Exclude) are ignored by PDC, TPS, and DV for cotrending and transit searches. In Sector 8, these cadences were identified using spacecraft telemetry from the fine pointing system. All cadences with pointing excursions >21 arcseconds (∼1 pixel) were flagged for manual exclude. Cadences at the start of orbit 24, before the instrument anomaly, were also marked with manual excludes because of complicated scattered light patterns and the relatively short time interval. See Figure 4 for an assessment of the performance of the cotrending based on the final set of manual excludes.

FFIs were only marked with bits 6 and 12 (Reaction Wheel Desaturation Events and Straylight). Only one FFI is affected by each momentum dump.

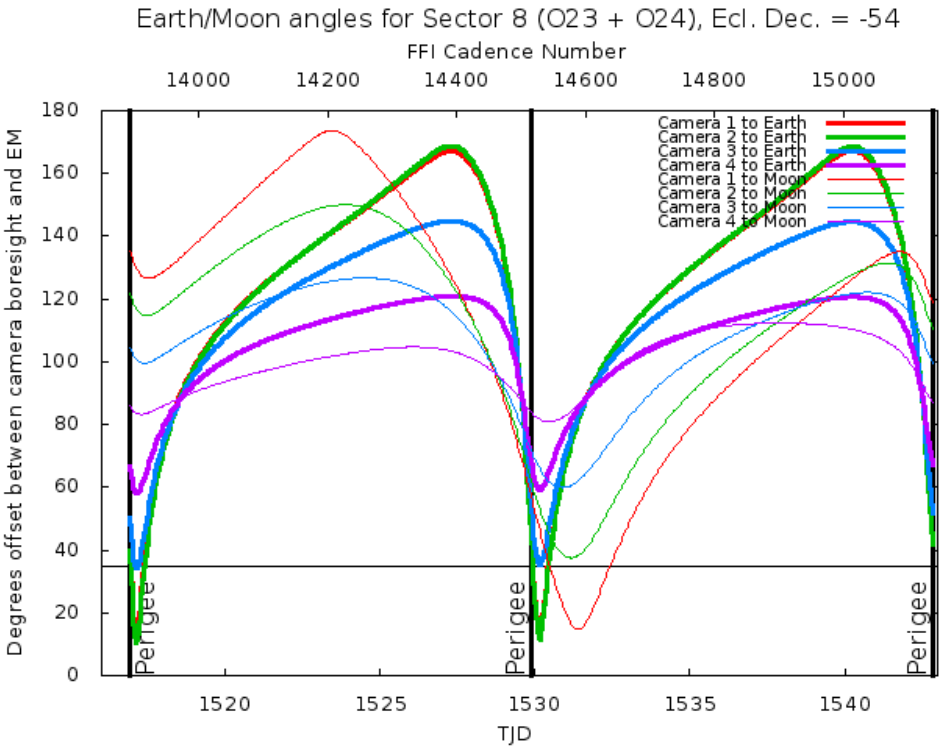

Figure 3: Angle between the four camera boresights and the Earth/Moon as a function of time. When the Earth/Moon moves within 37° of a camera's boresight, scattered light patterns and complicated features such as glints may appear. At larger angles, low level patchy features may appear. This figure can be used to identify periods affected by scattered light and the relative contributions of the Earth and Moon to the background. However, the background intensity and locations of scattered light features depend on additional factors, such as the Earth/Moon azimuth and distance from the spacecraft.

3 Anomalous Effects

3.1 Thermal Effects

Heaters were turned on after the instrument anomaly, increasing the camera temperature by $\sim 20°$ to approximately $-67°$ C. Once the camera power was restored, the heaters were turned off and the camera temperatures returned to nominal within three days. The temperature increase caused changes in the camera focal plane scale and mean black levels of individual CCD channels. The mean black levels are calibrated out in the SPOC pipeline. Changes in focal plane temperature cause changes in the raw photometry, but the PDC systematic error-correction algorithm removes this effect for most targets.

3.2 Smear Correction Issues

The following columns were impacted by bright stars in the the upper buffer rows, which bleed into the upper serial register resulting in an overestimated smear correction.

- Camera 4, CCD 3, Columns 1305-1315, Star Beta Doradus

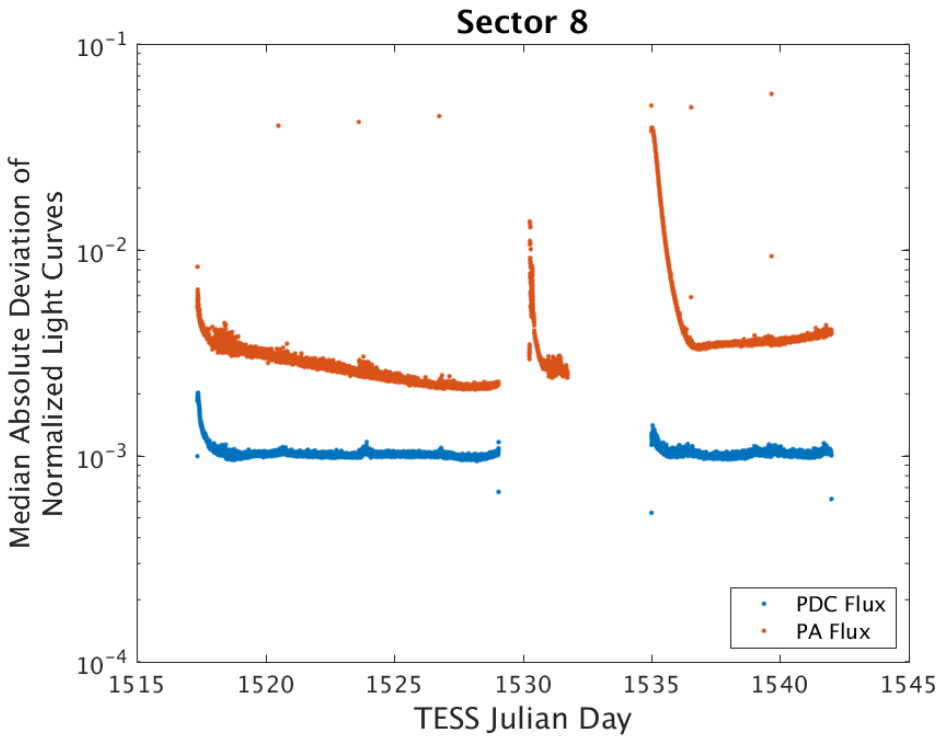

Figure 4: Median absolute deviation (MAD) for the 2-minute cadence data from Sector 8, showing the performance of the cotrending after identifying Manual Exclude data quality flags. The MAD is calculated in each cadence across stars with flux variations less than 1% for both the PA (red) and PDC (blue) light curves, where each light curve is normalized by its median flux value. The scatter in the PA light curves is much higher than that for the PDC light curves, and the outliers in the PA light curves are largely absent from the PDC light curves due to the use of the anomaly flags. Note that the first and last cadences in each orbit are treated as gaps by PDC.

3.3 Fireflies and Fireworks

Table 2 lists all firefly and fireworks events for Sector 8. These phenomena are small, spatially extended, comet-like features in the images that may appear one or two at a time (fireflies) or in large groups (fireworks). See the Instrument Handbook for a complete description.

3.4 Pixel Response Function

As of Sector 8, data processing used an updated pixel response function (PRF) model, derived from measurements taken with the improved pointing profile prior to the start of Sector 6.

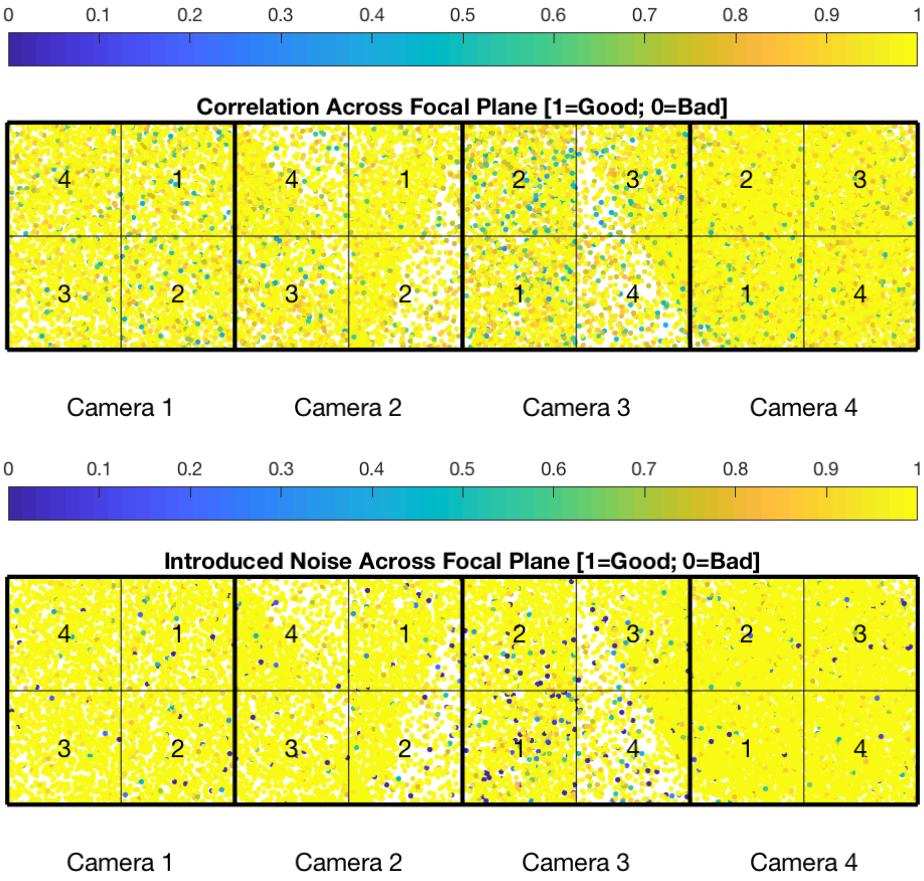

Figure 5: PDC residual correlation goodness metric (top panel) and PDC introduced noise goodness metric (bottom panel). The metric values are shown on a focal plane map indicating the camera and CCD location of each target. The correlation goodness metric is calibrated such that a value of 0.8 means there is less than 10% mean absolute correlation between the target under study and all other targets on the CCD. The introduced noise metric is calibrated such that a value of 0.8 means the power in broad-band introduced noise is only slightly above the level of uncertainties in the flux values.

4 Pipeline Performance and Results

4.1 Light Curves and Photometric Precision

Figure 5 gives the PDC goodness metrics for residual correlation and introduced noise on a scale between 0 (bad) and 1 (good). The performance of PDC is very good and generally uniform over most of the field of view. Figure 6 shows the achieved Combined Differential Photometric Precision (CDPP) at 1-hour timescales for all targets.

4.2 Transit Search and Data Validation

In Sector 8, the light curves of 19,994 targets were subjected to the transit search in TPS. Of these, Threshold Crossing Events (TCEs) at the 7.1σ level were generated for 772 targets.

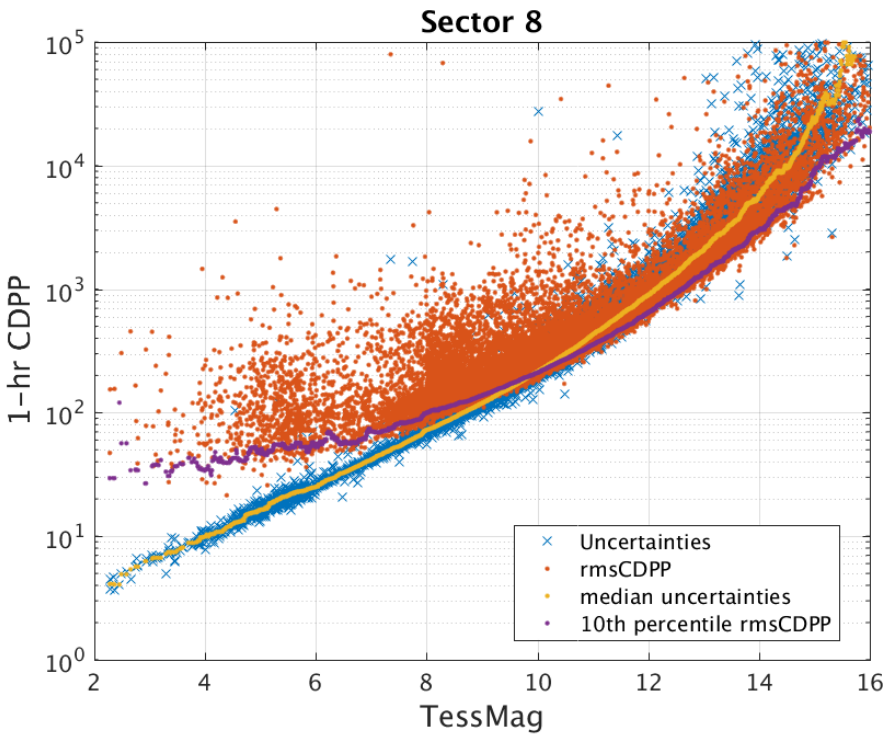

Figure 6: 1-hour CDPP. The red points are the RMS CDPP measurements for the 19,994 light curves from Sector 8 plotted as a function of TESS magnitude. The blue x's are the uncertainties, scaled to 1-hour timescale. The purple curve is a moving 10th percentile of the RMS CDPP measurements, and the gold curve is a moving median of the 1-hr uncertainties.

The top panel of Figure 7 shows the distribution of orbital periods for the TPS TCEs found in Sector 8. There is an excess of TCEs at orbital periods of 9 days and 17–18 days. Figure 8 shows the number of TCEs at a given cadence that exhibit a transit signal—the spacing between peaks accounts for the preferred periods in Figure 7. The 9 day excess is primarily caused by increased pointing jitter associated with the 2nd momentum dump and imperfect PDC corrections of the thermal impulse after the instrument anomaly. The 17–18 day excess is caused by imperfect corrections of the high level of scattered light at the start of orbit 23 and the thermal impulse after the instrument anomaly. Because of the difficulty of correcting the thermal impulse after the instrument anomaly, a data anomaly flag (bit 2, Safe Mode) was applied at the first cadence after data collection resumed—the

Table 2: Sector Fireflies and Fireworks

FFI Start	FFI End	Cameras	Description
2019051172935	2019051175935	3	Firefly
2019052222935	2019052225935	1	Firefly
2019053162935	2019053165935	2, 3	Firefly
2019058085935	2019058095935	2, 3	Fireflies

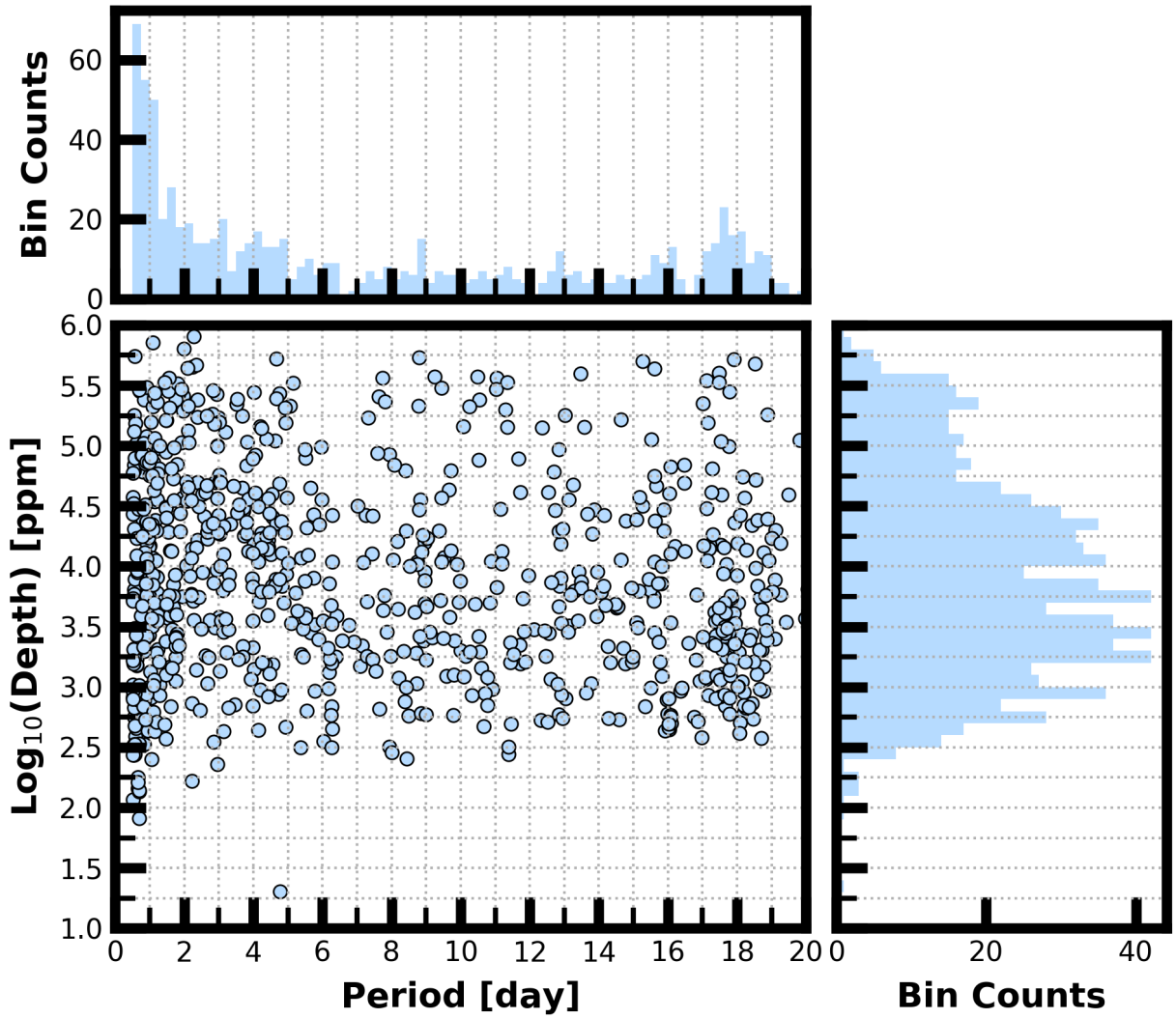

Figure 7: Lower Left Panel: Transit depth as a function of orbital period for the 1040 TCEs identified for the Sector 8 search. For enhanced visibility of long period detections, TCEs with orbital period <0.5 days are not shown. Reported depth comes from the DV limb darkened transit fit depth when available, and when not available, the DV trapezoid model fit depth. Top Panel: Orbital period distribution of the TCEs shown in the lower left panel. Right Panel: Transit depth distribution for the TCEs shown in the lower left panel.

flag indicates a period of time for which data are de-emphasized in the transit search and for which transits are excluded from difference images in data validation. This flag was only applied for the sake of the transit search and data validation; it otherwise has no meaning for mission operations in this sector.

The vertical histogram in the right panel of Figure 7 shows the distribution of transit depths derived from limb-darkened transiting planet model fits for TCEs. The model transit depths range down to the order of 100 ppm, but the bulk of the transit depths are considerably larger.

A search for additional TCEs in potential multiple planet systems was conducted in DV

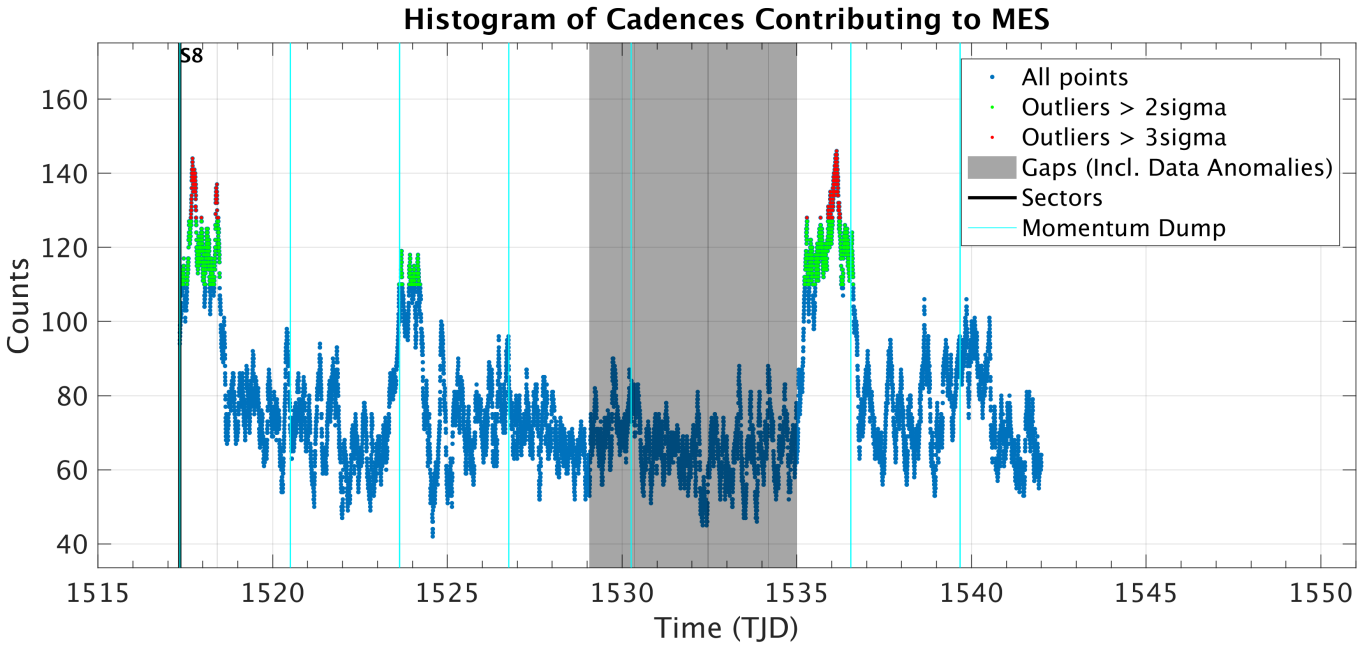

Figure 8: Number of TCEs at a given cadence exhibiting a transit signal. Isolated peaks are caused by a single event and result in spurious TCEs. The peaks typically align with pointing instabilities and strong background variations. Note that the flux time series are gapped between approximately TJD = 1529 and TJD = 1535.

through calls to TPS. A total of 1040 TCEs were ultimately identified in the SPOC pipeline on 772 unique target stars. Table 3 provides a breakdown of the number of TCEs by target. Note that targets with large numbers of TCEs are likely to include false positives.

Table 3: Sector 8 TCE Numbers

Number of TCEs	Number of Targets	Total TCEs
1	554	554
2	177	354
3	34	102
4	5	20
5	2	10
–	772	1040

References

Jenkins, J. M. 2017, Kepler Data Processing Handbook: Overview of the Science Operations Center, Tech. rep., NASA Ames Research Center

Jenkins, J. M., Twicken, J. D., McCauliff, S., et al. 2016, in Proc. SPIE, Vol. 9913, Software and Cyberinfrastructure for Astronomy IV, 99133E

Li, J., Tenenbaum, P., Twicken, J. D., et al. 2019, *PASP*, 131, 024506

Twicken, J. D., Catanzarite, J. H., Clarke, B. D., et al. 2018, *PASP*, 130, 064502

Vanderspek, R., Doty, J., Fausnaugh, M., et al. 2018, TESS Instrument Handbook, Tech. rep., Kavli Institute for Astrophysics and Space Science, Massachusetts Institute of Technology

Acronyms and Abbreviation List

BTJD Barycentric-corrected TESS Julian Date

CAL Calibration Pipeline Module

CBV Cotrending Basis Vector

CCD Charge Coupled Device

CDPP Combined Differential Photometric Precision

COA Compute Optimal Aperture Pipeline Module

CSCI Computer Software Configuration Item

CTE Charge Transfer Efficiency

Dec Declination

DR Data Release

DV Data Validation Pipeline Module

DVA Differential Velocity Aberration

FFI Full Frame Image

FIN FFI Index Number

FITS Flexible Image Transport System

FOV Field of View

FPG Focal Plane Geometry model

KDPH Kepler Data Processing Handbook

KIH Kepler Instrument Handbook

KOI Kepler Object of Interest

MAD Median Absolute Deviation

MAP Maximum A Posteriori

MAST Mikulski Archive for Space Telescopes

MES Multiple Event Statistic

NAS NASA Advanced Supercomputing Division

PA Photometric Analysis Pipeline Module

PDC Pre-Search Data Conditioning Pipeline Module

PDC-MAP Pre-Search Data Conditioning Maximum A Posteriori algorithm

PDC-msMAP Pre-Search Data Conditioning Multiscale Maximum A Posteriori algorithm

PDF Portable Document Format

POC Payload Operations Center

POU Propagation of Uncertainties

ppm Parts-per-million

PRF Pixel Response Function

RA Right Ascension

RMS Root Mean Square

SAP Simple Aperture Photometry

SDPDD Science Data Product Description Document

SNR Signal-to-Noise Ratio

SPOC Science Processing Operations Center

SVD Singular Value Decomposition

TCE Threshold Crossing Event

TESS Transiting Exoplanet Survey Satellite

TIC TESS Input Catalog

TIH TESS Instrument Handbook

TJD TESS Julian Date

TOI TESS Object of Interest

TPS Transiting Planet Search Pipeline Module

UTC Coordinated Universal Time

XML Extensible Markup Language